# Non-uniform interpolatory subdivision based on local interpolants of minimal degree

Kęstutis Karčiauskas[a] and Jörg Peters[b]

[1] Vilnius University, Lithuania,
[2] University of Florida, USA,
jorg@cise.ufl.edu

**Abstract.** This paper presents new univariate linear non-uniform interpolatory subdivision constructions that yield high smoothness, $C^3$ and $C^4$, and are based on least-degree spline interpolants. This approach is motivated by evidence, partly presented here, that constructions based on high-degree local interpolants fail to yield satisfactory shape, especially for sparse, non-uniform samples. While this improves on earlier schemes, a broad consideration of alternatives yields two technically simpler constructions that result in comparable shape and smoothness: careful pre-processing of sparse, non-uniform samples and interlaced fitting with splines of increasing smoothness. We briefly compare these solutions to recent non-linear interpolatory subdivision schemes.

## 1 Introduction

For non-uniformly spaced samples, uniform linear interpolatory curve subdivision algorithms [DL02,Sab10] often results in dramatic overshoot and oscillation. Starting with [War95], non-uniform constructions have been proposed such that new knots are inserted at the midpoints of knot-intervals. Mid-point insertion yields locally uniform knot spacings that meet at the original data points. The data points thereby become isolated 'extraordinary points' where left and right knot intervals may differ; and extraordinary point neighborhoods become the focus of the analysis. Recent examples of such non-uniform constructions are the edge parameter subdivisions [BCR11b,BCR11a] and $C^1$, $C^2$, $C^3$ and $C^4$ interpolatory curves [KP13b].

However, for higher smoothness, even these new non-uniform constructions exhibit shape problems for non-uniform data such as shown in Fig. 2a, pointing to the classical trade-off between smoothness, convexity and interpolation (cf. Fig. 10(c)). For example Warren's $C^2$ 6-point scheme [War95] as well as a $C^3$ 6-point scheme of [KP13b] unexpectedly loose the convexity of the piecewise linear interpolant to the samples (see Fig. 1c (top)); and a $C^4$ 10-point scheme visibly oscillates. By contrast the Catmull-Rom-inspired construction $\mathrm{CR}^2_{3/256}$ ( see Fig. 1 for the meaning of super-and subscripts) fares considerably better. We think these and many other examples indicate that large support, resulting from high-degree interpolants, causes problems and not just because of the increased complexity of the rules. To wit, Warren's scheme is based on local polynomial interpolants of degree 5, the $C^3$ 6-point scheme uses interpolants of degree 5 and 3 and the 10-point scheme polynomials of degree 7 – whereas the $\mathrm{CR}^2_{3/256}$ construction is based on local interpolants of degree 2.

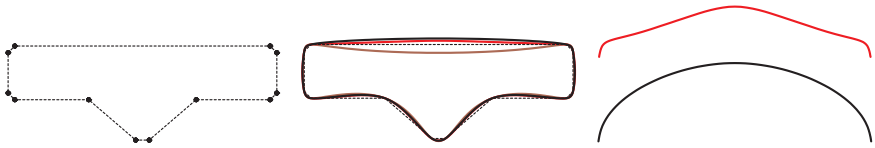

(a) input polygon (b) 3 interpolants (c) part scaled by 10 in $y$

**Fig. 1. Thumb tag** data. The constructions use centripetal knot spacing [Lee89] since, for non-uniform samples, centripetal is superior to chordal. (b) brown = 10-point scheme of [KP13b] with $w = 0.00098$, dipping down in the center; black = Catmull-Rom $C^2$ construction $\mathrm{CR}^2_{3/256}$ ( *The notation of [KP13b] exposes, in the superscript, continuity and possibly the degrees of local interpolants and, in the subscript the setting of the free parameter $w$ of the construction*); red = $C^3$ 6-point scheme $\mathrm{A}^{3,5:3:3}_{0.0141}$ visually identical to $\mathrm{A}^{2,5:3}_{3/256}$, i.e. Warren's $C^2$ 6-point scheme[War95]. (c) The roofs of the T-shaped polygon of $\mathrm{A}^{2,5:3}_{3/256}$ (top) and $\mathrm{CR}^2_{3/256}$ (bottom) are displayed with different offset for clarity and scaled by 10 in the $y$ direction to emphasize the curvature oscillation of $\mathrm{A}^{2,5:3}_{3/256}$.

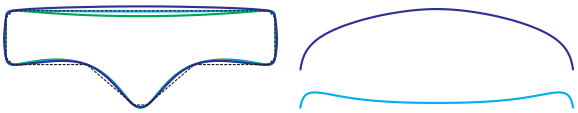

(a) new interpolants (b) scaled by 10 in $y$

**Fig. 2.** Minimal degree $d$ local interpolant constructions: blue = $C^3$ 6-point, $d = 3$; cyan = almost $C^4$ 8-point, $d = 4$; green = $C^4$ 10-point, $d = 4$.

While reproduction of polynomials of degree $k$ is important for approximation, minimal degree of the interpolants seems consistently advantageous both for controlling shape and for simplicity of downstream use. Hence, in this paper, we construct new $C^3$ and $C^4$ non-uniform schemes using only the local interpolants of minimal degree $d = 3, 4$. Indeed, the construction using $d = 3$ clearly improves on earlier schemes. But $d = 4$ interpolants used in a new 8-point scheme of Hölder regularity $> 3.96$ as well as in a $C^4$ 10-point scheme, provide only slight improvement and loose convexity for highly non-uniform data. By contrast, as illustrated in Fig. 2, the curve generated by the 6-point scheme with $d = 3$ preserves the expected convexity.

This partial failure led us to explore a broader set of alternatives: initial refinement of data with lower-order schemes followed by higher-order schemes to achieve the required smoothness; and, secondly, interlaced fitting with splines of increasing smoothness. We also consider, in Section 4.2, locally-determined knot spacings that reduce th enon-uniformity by spreading it out.

For ease of comparison, we illustrate all our experiments with curves derived from the 'thumb tag' data Fig. 1(a). Many other data sets were tested with like results, e.g. the 'bread loaf' data of Fig. 10(a).

*Structure of the paper* Section 2 reviews the analysis of non-uniform interpolatory midpoint-insertion subdivision schemes of [KP13b] adding improved techniques to

establish Rouché's Theorem for subdivision from low-degree interpolants. Section 3 presents new non-uniform $C^3$ and $C^4$ subdivision constructions based on least-degree spline interpolants. Section 4 contrasts them with alternative constructions: careful pre-processing of sparse, non-uniform samples and interlaced fitting with splines of increasing smoothness. Section 4.4 and Section 4.5 develop remedies for fast changing discrete curvature and Section 5 comments on the minimality of the interpolants.

## 2 Non-uniform symmetric interpolatory midpoint subdivision

Except for Section 2.1, this section closely follows the exposition of [KP13b]. Given a sequence of increasing scalars $\{t_i\}$, called knots, and a sequence of points $\{\mathbf{p}_i\}$ in $\mathbf{R}^d$, the $k+1$st point sequence is derived from the $k$th, starting with $\mathbf{p}_i^0 := \mathbf{p}_i$, by

$$\mathbf{p}_{2i}^{k+1} := \mathbf{p}_i^k \ , \quad \mathbf{p}_{2i+1}^{k+1} := \sum_{j=1}^{2n} e_{ij}\mathbf{p}_{i-n+j}^k. \tag{1}$$

That is, in every refinement step, we insert one new point between two old ones. The $2n$ coefficients $e_{ij}$ depend on $2n-2$ scalars $\beta_{i-n+2},\dots,\beta_{i+n-1}$ that in turn depend on the knots via $\beta_i := \frac{t_{i+1}-t_i}{t_i-t_{i-1}}$, the ratio of the adjacent knot intervals. In the following, new knots are picked as midpoints of intervals $t_{2i+1}^{k+1} := \frac{1}{2}(t_i^k + t_{i+1}^k), t_{2i}^{k+1} := t_i^k$, a choice that [DGS99] calls semi-regular. Therefore

$$\beta_{2i}^{k+1} := \beta_i^k, \quad \beta_{2i+1}^{k+1} := 1. \tag{2}$$

All constructions will be invariant under the replacements
symmetry: $e_{ij} \to e_{i,2n+1-j}$ $\beta_{i-n+2+s} \to (\beta_{i+n-1-s})^{-1}$,
translation: $e_{ij} \to e_{i+s,j}$ $\quad \beta_{i-n+2},\dots,\beta_{i+n-1} \to \beta_{i-n+2+s},\dots,\beta_{i+n-1+s}$.
As in [KP13b], we follow [War95] and first establish the smoothness in the uniform case $\beta_i = 1$, then focus on the extraordinary points corresponding to an isolated $\beta \neq 1$.

For uniform knots $\beta_i = 1$ for all $i$ and we may abbreviate the coefficients to $\bar{e}_j$. Since $\bar{e}_{2n-i} = \bar{e}_i$ for the schemes in this paper, Table 1 displays only $\bar{e}_j$, $j = 1,\dots,n$ of the relevant generalizations of the classical 4-point scheme. The uniform schemes are analyzed using z-transforms, see [Dyn92,DL02,DFH04].

**Table 1.** Uniform symmetric $C^{n-1}$ $2n$-point interpolatory schemes with parameter $w$ [Wei90,KLY07].

| $2n$ | $\bar{e}_j, j = 1,\dots,n$ | $C^{n-1}$ range for $w$ |
|---|---|---|
| 6 | $w, -3w - \frac{1}{16}, 2w + \frac{9}{16}$ | $(0\,..\,0.042]$ |
| 8 | $-w, 5w + \frac{3}{256}, -9w - \frac{25}{256}, 5w + \frac{75}{128}$; | $[0.0016\,..\,0.0084]$ |
| 10 | $w, -7w - \frac{5}{2048}, 20w + \frac{49}{2048}, -28w - \frac{245}{2048}, 14w + \frac{1225}{2048}$ | $[0.0005\,..\,0.0016]$ |

The now isolated non-uniform locations are analyzed by the following four steps of which especially the last benefits from symbolic computation.

1. Repeated knot insertion at the middle of intervals surrounds each knot where $\beta \neq 1$ by knots with $\beta = 1$. The $\beta$ at this isolated extraordinary knot is denoted $\gamma$ in the following.
2. Uniform subdivision applies where $\beta = 1$. Table 1 gives the $w$-ranges for $C^m$ continuity.
3. The $(4n-1) \times (4n-1)$ subdivision matrix $L$ for the isolated extraordinary point has the rows

$$\begin{aligned} L_1 &:= (E_0, \mathbf{0}^{2n-1}); \quad L_{4n-1} := (\mathbf{0}^{2n-1}, E_0); \\ L_{2i} &:= (\mathbf{0}^{n-1+i}, 1, \mathbf{0}^{3n-1-i}) \ , \ i = 1, \ldots, 2n-1, \\ L_{2i+1} &:= (\mathbf{0}^{i}, E_i, \mathbf{0}^{2n-1-i}) \ , \ i = 1, \ldots, 2n-2, \end{aligned} \tag{3}$$

   where $\mathbf{0}^s$ is a sequence of $s$ zeros,

$$E(\beta_{i-n+2}, \ldots \beta_{i+n-1}) := (e_{i1}, \ldots, e_{i,2n}),$$

   maps the $2n-2$ ratios $\beta$ to the $2n$ coefficients $e_{ij}$, and, with $\mathbf{1}^s$ a sequence of $s$ ones, $E_k := E(\mathbf{1}^{2n-2-k}, \gamma, \mathbf{1}^{k-1})$, $k = 1, \ldots, 2n-2$, $E_0 := E(\mathbf{1}^{2n-2})$. For an example see e.g. [War95, Sec.5].
   Since the constructions are chosen to reproduce polynomials up to degree $m$, the matrix $L$ has eigenvalues $1, \frac{1}{2}, \ldots, \frac{1}{2^m}$ whose eigenfunctions are the polynomials $1, t, \ldots, t^m$. For analysis, the characteristic polynomial $\chi(\lambda)$ of $L$ is best factored into

$$\chi(\lambda) = const(\lambda - 1)(\lambda - \frac{1}{2}) \cdots (\lambda - \frac{1}{2^m})\ell(\lambda)r(\lambda), \tag{4}$$

   where $\ell(\lambda)$ is of the form $(\lambda \pm w)^k$ that allows immediate checking whether its roots are strictly *dominated* in absolute value by $\frac{1}{2^m}$. To establish smoothness, it then suffices to show that the absolute values of the roots of $r(\lambda)$ are dominated, i.e. strictly less than $\frac{1}{2^m}$.
4. Note that the polynomial $r(\lambda)$ also depends on the extraordinary ratio $\gamma$ and the parameter $w$. We pick a suitable candidate value $w$ after numerical experiments. To prove that the roots of the polynomial $r(\lambda)$ are dominated by $\underline{\lambda} := \frac{1}{2^m}$, we use Rouché's Theorem [Lan85] in the following way.
   a. Let $\tilde{r}(\lambda)$ be the polynomial obtained by replacing $\gamma \to \frac{1}{\gamma}$. By checking that $\tilde{r}(\lambda)\gamma^{\tilde{m}} = r(\lambda)$ for some $\tilde{m}$, we may assume that $\gamma \in (0, 1]$.
   b. $r(\lambda) := \sum_{s=0}^{p} d_s(\gamma)\lambda^s$ has coefficients $d_s(\gamma)$ that are themselves polynomials (with Bézier coefficients $d_i^s$) of degree $k$ over $[0, 1]$.
   c. We check, separately for each $i$, by symbolic computation that

$$\sum_{s=0}^{p-1} |d_i^s|\bar{\lambda}^s - d_i^p\bar{\lambda}^p < 0, \quad d_i^p > 0 \, . \tag{5}$$

   Let $g(z) := \sum_{s=0}^{p} d_s(\gamma)z^s$ and $h(z) := d_p(\gamma)z^p$ for $z$ on a circle of radius $\bar{\lambda}$. Then (5) implies the strict inequality in

$$|g(z) - h(z)| = |\sum_{s=0}^{p-1} d_s z^s| \leq \sum_{s=0}^{p-1} |d_s||z^s| < |h(z)|.$$

Rouché's Theorem [Lan85] implies that $g$ and $h$ have the same number $p$ of roots in the $\bar{\lambda}$-disk, i.e. by the degree of $g$ all roots of $g$ are confined to the $\bar{\lambda}$-disk and hence $r(\lambda)$ is dominated by $\bar{\lambda}$.

### 2.1 Details of proving root domination

Compared to constructions based on higher-degree interpolants, our minimal degree constructions have a smaller, easily checked factor $\ell(\lambda)$ but a more complex factor $r(\lambda)$. Using Rouché's Theorem, we show that the roots of the polynomial $r(\lambda)$ are dominated by $\bar{\lambda} > \underline{\lambda} := 1/2^m$, where $\bar{\lambda} = 1/5$ for the 6-point $C^3$ scheme of Section 3.1, $\bar{\lambda} = 1/7$ for the 8-point almost $C^4$ scheme of Section 3.2 and $\bar{\lambda} = 1/8$ for the 10-point $C^4$ scheme of Section 3.3.

To show that the roots of $r(\lambda)$ are dominated by $\underline{\lambda}$, $r(z)$ is considered as a complex function over the annulus $\underline{\lambda} \le |z| \le \bar{\lambda}$, $z := x + \mathbf{i}y$. We define $F_1(x, y) := |r(z)|^2$ and $F_2(x, y) := F_1(-y, x)$ and parameterize the positive quarter-annulus by

$$\rho := (\underline{\lambda}(1-u) + \bar{\lambda}u)\Big(\frac{1-v^2}{1+v^2}, \frac{2v}{1+v^2}\Big), \quad (u, v) \in [0\,..\,1]^2.$$

We further define $f_i(u, v, \gamma) := F_i \circ \rho(u, v)$, $i = 1, 2$. After scaling the denominator by $(1 + v^2)^d$, $f_i$ becomes a polynomial (of high degree) in the variables $(u, v, \gamma)$. It is converted to trivariate Bézier form. By looking at the coefficients, we can verify (in Section 3.1 3.2, 3.3) that these $f_i$ and hence the functions $F_1$, $F_2$ are strictly positive. The proof for the other two quadrants not covered by $f_i$ then follows by substituting the complex conjugate $z \to \bar{z}$ and observing that $r(z)$ has real coefficients.

## 3 Highly smooth non-uniform interpolatory subdivision

This section presents three constructions that yield respectively $C^3$, almost $C^4$ and $C^4$ curves. Denoting by $\mathbf{f}_i^k$ the polynomial of degree $k$ that interpolates, for $s = 0, \ldots, k$, the points $\mathbf{p}_{i-\kappa+s}$ at the values $t_{i-\kappa+s}$, $\kappa := \lfloor \frac{k}{2} \rfloor$, we define the localized interpolant to be

$$\breve{\mathbf{f}}_{i,j}^k(u) := \mathbf{f}_j^k((1-u)t_i + ut_{i+1}),\ u \in [0\,..\,1]. \tag{6}$$

### 3.1 $C^3$ 6-point scheme from cubic interpolants

*Construction of new points* $\tilde{\mathbf{p}}_{2i+1}$

1. The interpolating curves $\breve{\mathbf{f}}_{i,i-1}^3$, $\breve{\mathbf{f}}_{i,i}^3$ and $\breve{\mathbf{f}}_{i,i+1}^3$ of degree 3 are expressed in Bézier form of degree 5 with coefficients $\mathbf{b}_k^l$, $\mathbf{b}_k^m$, $\mathbf{b}_k^r$, $k = 0, \ldots, 5$.
2. The Bézier coefficients $\mathbf{b}_k$ of a degree 5 curve $\mathbf{g}$ are defined as

$$\mathbf{b}_k := \frac{\mathbf{b}_k^l + \mathbf{b}_k^m}{2}, k = 0, 1, 2; \quad \mathbf{b}_k := \frac{\mathbf{b}_k^r + \mathbf{b}_k^m}{2}, k = 3, 4, 5.$$

3. Set

$$\tilde{\mathbf{p}}_{2i+1} := \tilde{\omega}\mathbf{g}(\frac{1}{2}) + (1-\tilde{\omega})(\frac{1}{12}(\mathbf{b}_0 + \mathbf{b}_5) + \frac{5}{12}(\mathbf{b}_2 + \mathbf{b}_3)),$$

$$\tilde{\omega} := 16 - 1152w,\ w := \frac{5}{384} \approx 0.01302.$$

*Analysis* The analysis via z-transforms confirms that the construction for uniform knots is $C^3$. Since $\ell(\lambda) = (\lambda - w)^2$, we only needed to analyze the degree 5 polynomial $r(\lambda)$ according to Section 2.1 to confirm $C^3$ continuity. All Bézier coefficients of $f_2$ are strictly positive. Proving strict positivity of $f_1$ is only possible after subdividing the domain $[0\,..\,1]^3$ in the $u$- and $\gamma$-directions as shown in Fig. 3: The restriction of $f_1$ to each of the subdomains has strictly positive Bézier coefficients.

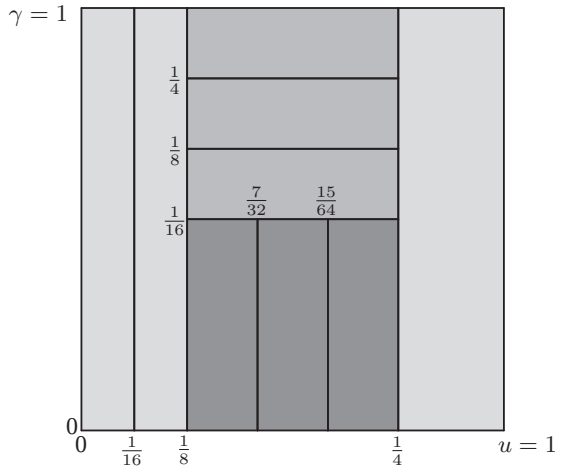


**Fig. 3.** Subdivision of the $(u, \gamma)$ coordinates of $f_1$ to prove strict positivity and hence $C^3$ continuity of the new 6-point scheme.

*Comparison* The global shape improvement over the $C^3$ schemes from [KP13b] can be observed in Fig. 2.

### 3.2 An almost $C^4$ 8-point scheme

*Construction of new point* $\tilde{\mathbf{p}}_{2i+1}$
1. We set $\mathbf{p}^l := \mathbf{f}^4_{i-1}(et_{i-1} + (1-e)t_i)$, $\mathbf{p}^r := \mathbf{f}^4_{i+2}((1-e)t_{i+1} + et_{i+2})$.
2. By $\mathbf{f}^l$ and $\mathbf{f}^r$ we denote degree 4 polynomials that interpolate respectively

$$\begin{aligned}
&\mathbf{f}^l(t_{i-1}) = \mathbf{p}_{i-1},\ \mathbf{f}^l(et_{i-1} + (1-e)t_i) = \mathbf{p}^l,\ \mathbf{f}^l(t_i) = \mathbf{p}_i,\\
&\mathbf{f}^l(t_{i+1}) = \mathbf{p}_{i+1},\ \mathbf{f}^l(t_{i+2}) = \mathbf{p}_{i+2},\\
&\mathbf{f}^r(t_{i-1}) = \mathbf{p}_{i-1},\ \mathbf{f}^r(t_i) = \mathbf{p}_i,\ \mathbf{f}^r(t_{i+1}) = \mathbf{p}_{i+1},\\
&\mathbf{f}^r((1-e)t_{i+1} + et_{i+2}) = \mathbf{p}^r,\ \mathbf{f}^r(t_{i+2}) = \mathbf{p}_{i+2}.
\end{aligned}$$

3. Set

$$\begin{aligned}
\tilde{\mathbf{p}}_{2i+1} :=& \tilde{\omega}\frac{1}{2}(\mathbf{f}^4_i + \mathbf{f}^4_{i+1})(\frac{t_i + t_{i+1}}{2}) + (1-\tilde{\omega})\frac{1}{2}(\mathbf{f}^l + \mathbf{f}^r)(\frac{t_i + t_{i+1}}{2}), \qquad (7)\\
\tilde{\omega} :=& \frac{1}{3(2-e)}(6 - 3e - 256we - 512w).
\end{aligned}$$

*Analysis* For a uniform knot sequence, $e$ cancels out. For the choice $w := 0.0038$, the analysis via z-transforms confirms that the construction for uniform knots is $C^3$. Careful numerical treatment shows that Hölder regularity exceeds $3.96$ and that a nearby value of $w$ yields an upper bound of $4.04$ [Hor12]. That is, the analysis neither confirms $C^4$ continuity nor does it rule out $C^4$ continuity.

Analysis of the non-uniform case yields $\ell(\lambda) = (\lambda + w)^2$ and $r(\lambda)$ of degree 8. The analysis of Section 2.1 shows that this scheme can be $C^4$ for $e := \frac{1}{4}$ and $w := 0.0038$, if the uniform scheme is $C^4$. Specifically, all Bézier coefficients are strictly positive for $f_2$ and the restrictions of the $u$-range of $f_1$ to subintervals $(0, \frac{1}{32}, \frac{1}{16}, \frac{1}{8}, \frac{1}{4}, \frac{1}{2}, 1)$ yields strictly positive Bézier coefficients, hence also positive $f_1$.

### 3.3 $C^4$ 10-point scheme from quartic interpolants

We use the 8-point scheme of Section 3.2 for this construction.

*Construction of new point* $\tilde{\mathbf{p}}_{2i+1}$
1. We set $\mathbf{p}^l := \mathbf{f}^4_{i-2}(et_{i-3} + (1-e)t_{i-2})$, $\mathbf{p}^r := \mathbf{f}^4_{i+3}((1-e)t_{i+3} + et_{i+4})$, where $e := \frac{5-2048w}{5+6144w}$.
2. We set $\tilde{e} := \frac{1}{2}$, $\tilde{w} := 2w + \frac{5}{2048}$,
3. The point $\tilde{\mathbf{p}}_{2i+1}$ is then defined by the 8-point scheme of Section 3.2 with parameters $\tilde{e}$ and $\tilde{w}$ and auxiliary points and knots

$$\begin{array}{cccccccc} \mathbf{p}^l & & \mathbf{p}_{i-2} & \mathbf{p}_{i-1} & \mathbf{p}_i & \mathbf{p}_{i+1} & \mathbf{p}_{i+2} & \mathbf{p}_{i+3} & \mathbf{p}^r \\ et_{i-3} + (1-e)t_{i-2} & & t_{i-2} & t_{i-1} & t_i & t_{i+1} & t_{i+2} & t_{i+3} & (1-e)t_{i+3} + et_{i+4} \end{array}$$

*Analysis* The standard analysis of Section 2 yields $\ell(\lambda) = (\lambda - w)^2$ and $r(\lambda)$ of degree 12. For our choice of $w = 0.0014$, the analysis described in Section 2.1 yields that all Bézier coefficients are strictly positive and hence $f_i > 0$.

*Comparison* While the new 10-point construction improves the global shape compared to the 10-point scheme in Fig. 1, the improvement is not impressive and the global shape is worse than that of the almost $C^4$ 8-point scheme that is also based on quartic interpolants but has smaller support.

## 4 Alternative approaches to improve quality

Given the lack of decisive improvement for $C^4$ continuity, we explored a broader set of alternatives to deal with highly non-uniform data.

### 4.1 $C^2$ 6-point preparation

The simple $C^2$ 6-point interpolatory scheme $\mathrm{CR}^2_{\mathrm{w}}$ of [KP13b] consistently exhibits a good global shape with the choice $w = 3/256$ yielding a better curvature distribution than another natural choice $w = 1/192$, see Fig. 4b,c. Wide support and degree interpolants that exhibit poor global shape for highly non-uniform samples benefit from

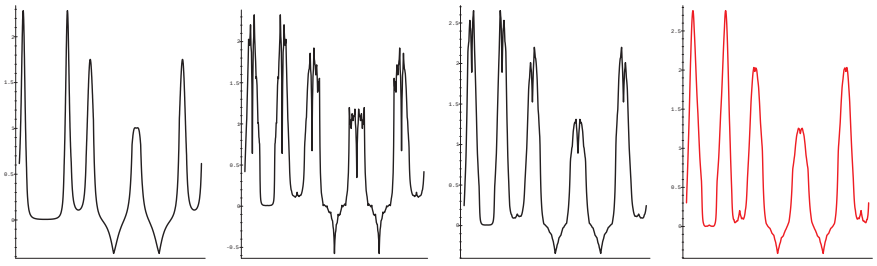

(a) $C^2$ spline (b) $\mathrm{CR}^2_{1/192}$ (c) $\mathrm{CR}^2_{3/256}$ (d) $\mathrm{CR}^2_{3/256}$ + $\mathrm{A}^{2,5:3}_{3/256}$

**Fig. 4.** Curvature plots. Visually all curves are similar to $\mathrm{CR}^2_{3/256}$ shown as black curve in Fig. 1b. (a) $C^2$ Catmull-Rom spline [KP13b] from which are derived (b) $\mathrm{CR}^2_{1/192}$ and (c) $\mathrm{CR}^2_{3/256}$. (c) has better curvature distribution and is used for preparation. (d) one step of $\mathrm{CR}^2_{3/256}$ followed by $\mathrm{A}^{2,5:3}_{3/256}$ thereafter.

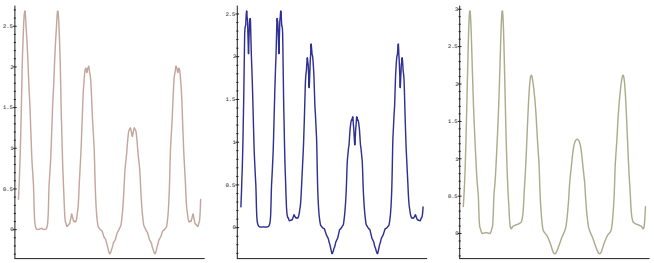

(a) 6-point $\mathrm{A}^{3,5:3:3}_{0.0141}$ (b) new $C^3$ scheme (c) 8-point from [KP13b], $w = 0.0038$

**Fig. 5.** Curvature of $C^3$ subdivision curves after preparation with $\mathrm{CR}^2_{3/256}$.

applying a single initial step of $\mathrm{CR}^2_{3/256}$. After this *6-point preparation*, the curves generated by the schemes improve both in global shape and in curvature distribution, to a degree usually observed only for uniformly distributed data. For example, 6-point preparation of the inferior 10-point scheme of [KP13b] in Fig. 6a demonstrates that a curvature distribution can be achieved, as good as for the new 10-point scheme Fig. 6b. The 6-point preparation also dramatically improves the red curve in Fig. 1c to a curve visually identical to $\mathrm{CR}^2_{3/256}$ but with better curvature distribution. We note that repeated pre-processing leaves the global shape visually unchanged but appears to harm the curvature distribution (Fig. 6c,d).

### 4.2 Equalizing knots disappoint

By inserting the knots to make the spacing more uniform, we hoped to maintain curvature quality while switching from complicated non-uniform rules to simple uniform

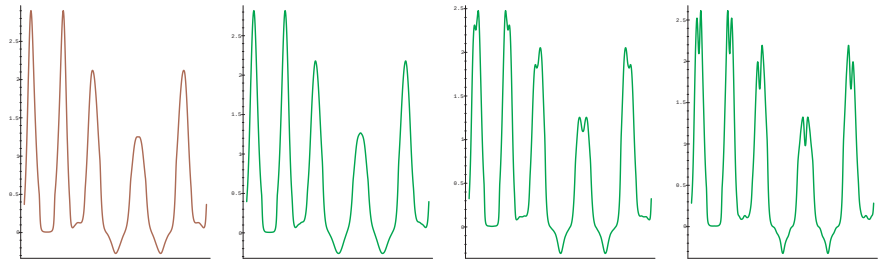

(a) $\mathrm{CR}^2_{3/256}$ + [KP13b] (b) new 10-point (c) 2 steps (d) 3 steps

**Fig. 6.** Curvature plots of $C^4$ 10-point subdivision curves after $\mathrm{CR}^2_{3/256}$ preparation: (a) 10-point, $w = 0.00098$ from [KP13b] after one step of $\mathrm{CR}^2_{3/256}$; (b) one (c) two (d) three steps followed by new 10-point scheme.

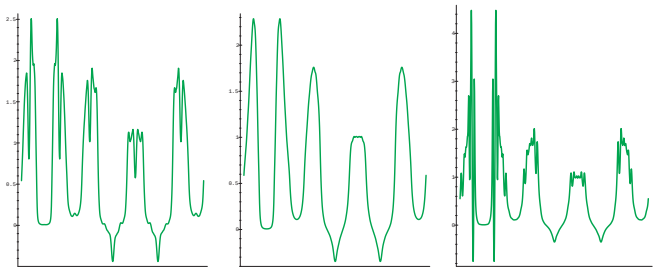

(a) $\mathrm{CR}^2_{1/192}$ equalizing + 10 point (b) Equalized $cr^2_1$ spline (c) uniform completion

**Fig. 7.** Curvature plots. (a) new 10-point scheme after three steps of $\mathrm{CR}^2_{1/192}$ to equalize knots; (b) Three steps of equalized sampling othe $C^2$ spline $cr^2_1$ of [KP13b]. (c) uniform 10-point scheme ($w = 0.0014$) after 4 steps of equalizing sampling of $C^2$ spline.

ones. We applied up to three steps of the adaptive $\mathrm{CR}^2_{3/256}$ construction of [KP13b] to be able to define new points with equalizing knots according to [SD05]:

$$t^{k+1}_{2i+1} := (1-\bar{t})t^k_i + \bar{t}t^k_{i+1},\ \bar{t} := \frac{\sqrt{t^k_{i+1} - t^k_{i-1}}}{\sqrt{t^k_{i+1} - t^k_{i-1}} + \sqrt{t^k_{i+2} - t^k_i}}. \tag{8}$$

However Fig. 7a illustrates that equalizing, followed by the new 10-point scheme, only harms the curvature distribution shown in Fig. 4c. (A referee has suggested that this follows from the lack of curvature continuity of the curves generated in [SD05], as recently shown in [FBCR1x]).

Several equalizing upsampling steps of a quartic $C^2$ spline (see Fig. 4a) shows no improvement in Fig. 7b despite increased effort. Subsequent uniform 10-point subdivision when the knot interval ratios are close to 2 clearly yields no progress; see Fig. 7c.

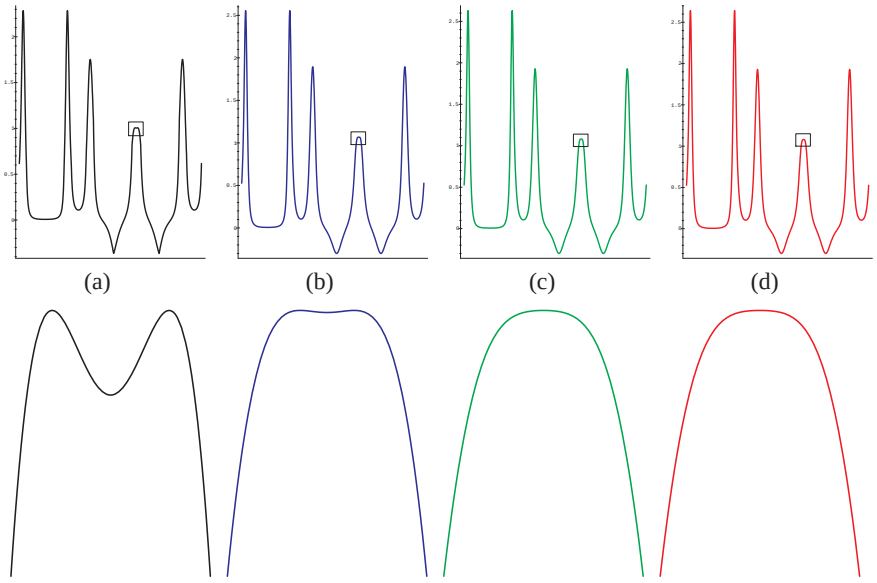


**Fig. 8.** (*top*) Curvature plots (visually the splines are hard to distinguish). (*bottom*) magnified vicinity of curvature distribution marked by the box in the respective top figure. Note, (a) is the same as Fig. 4(a). (b): $C^2$ spline (a) smoothed to $C^3$; (c): $C^3$ spline (b) smoothed to $C^4$; (d): $C^4$ spline (c) smoothed to $C^5$.

### 4.3 Subdivision tracking repeated-smoothing-interpolating splines

[KP13b] introduced the idea of interlaced smoothing of interpolatory splines. Initially splines of low continuity and degree determine the global shape. Then the degree of these splines is raised and the additional degrees of freedom used to make the spline smoother, while still closely conforming to the initial shape. For example, we start with $C^1$ Catmull-Rom splines and express them as splines of degree 4. Then we smooth the spline, modifying the $C^1$ constraint and enforcing at the same time a new $C^2$ constraint to arrive at $C^2$ quartic splines. In a next step these $C^2$ quartic splines are raised to degree 6 followed by enforcing $C^2$ and $C^3$ constraints.

Interlacing degree-raising with smoothing is important for quality. Compared to immediately setting the degree and enforcing smoothness, interlacing yields better curvature distribution as demonstrated in [KP13b]; see Fig. 8, 9. New higher-order smoothing formulas for Fig. 8c,d are given in the Appendix. The progression of Fig. 8 typifies the beneficial effect of the smoothing process.

We can disguise the pure spline construction as a subdivision scheme by uniformly upsampling their Bézier segments as detailed in the Appendix Section 6.2, labelling each segment and inserting a new point at the middle of the interval. Spline construction plus upsampling amortizes over repeated subdivision steps so that after a few steps the approach is as efficient as simple uniform subdivision with higher continuities.

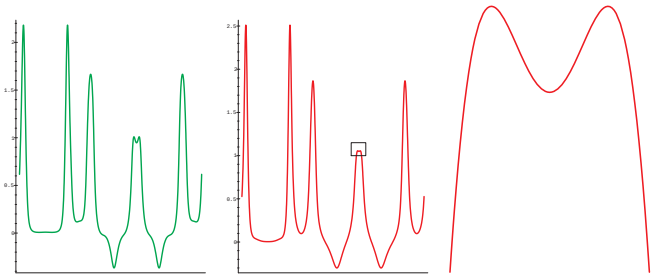

(a) (b) (c)

**Fig. 9.** Curvature plots. (a): $C^2$ spline from Fig. 8(a) smoothed to $C^4$; (b): $C^3$ spline from Fig. 8(b) smoothed to $C^5$; (c): magnified part of (b).

### 4.4 Relaxed interpolation

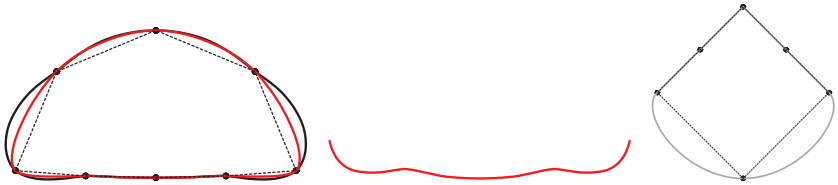

(a) 4pt, 4pt circle preserving (b) zoom of 4pt scheme (c) simple $C^1$ spline

**Fig. 10.** Interpolating $C^1$ curves. (a): red = 4-point scheme [DLG88], black = geometric (non-linear) circle preserving scheme from [DH12]; (b) vertical scaling of [DLG88] (also [DH12,SD05] visibly oscillates in (a)). (c) convex $C^1$ spline with collapsed control segment to deal with the classical trade-off between smoothness, convexity and interpolation, already present in the functional data $x_i = i, y_i = |i|, i \in -2, \ldots, 2$.

One of the motivations of geometric (non-linear) subdivision is reproduction of basic shapes, such as the circle. While this is achieved in pieces, the transition between pieces of different shape often suffers (Fig. 10a, 11a).

An alternative is relaxed interpolation [ADS10]. Relaxed interpolation is akin to quasi-interpolation and generally, compared to strict interpolation, improves the shape for mildly changing data. However, as the oscillation in Fig. 11a illustrates, even relaxation does not cope well with rapidly changing discrete curvature. For denser samples, the reproduction property of geometric subdivision improves the shape but transitions remain a challenge (see Fig. 11d).

### 4.5 Curvature-sensitive interpolation

Not all data admit interpolation by smooth, convex curves, especially where local discrete curvature changes rapidly, see Fig. 10c. For the specific case, we can modify $C^1$ spline interpolation to preserve interpolation and convexity, the natural requirements for fair curves. We then have to give up on geometric smoothness, for example by collapsing a control segment. More generally, quasi-interpolation with splines does not fare well unless it is made 'curvature-sensitive' [KP13a] as shown in Fig. 11b. We think that, without taking into account discrete local curvature of the input data, any curve construction, whether subdivision or splines, can and will oscillate. Since curvature-sensitive splines switch depending on local discrete curvature, we do not present a subdivision analog. Such an analogue is surely difficult to analyze, especially since rigorous proofs of smoothness of simpler non-linear, geometric subdivision are still a challenge. (For splines we have at least smoothness by construction.) We note that curvature-sensitive splines can be modified to reproduce a circle [KP12] as illustrated in Fig. 11e and that while cubic $C^2$ B-splines are indeed of high quality, quasi-interpolating (relaxed) curvature-sensitive splines are closer to the input data, see Fig. 11b.

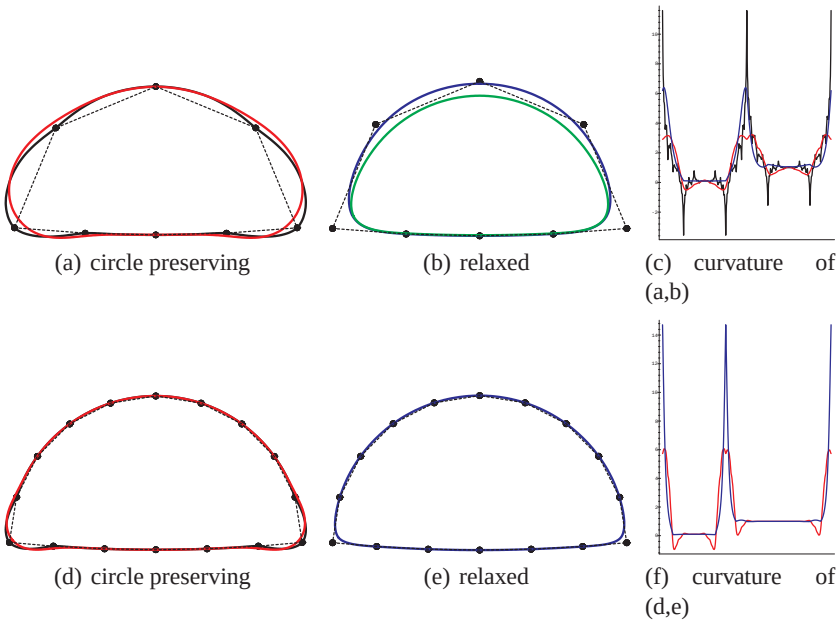

(a) circle preserving (b) relaxed (c) curvature of (a,b)

(d) circle preserving (e) relaxed (f) curvature of (d,e)

**Fig. 11.** Relaxed interpolation. (a,d) Non-linear subdivision curves: black = circle preserving [SD05], red = relaxed circle preserving [Sab10]. (b,e) blue = convex $C^2$ cubic, relaxed curvature-sensitive spline [KP13a], (b) green = cubic $C^2$ B-spline;

## 5 Least degree

In our title and later on, we refer to interpolants of 'minimal degree' and give a rationale for seeking low degree. Indeed, our schemes use the natural midpoint insertion that generates piecewise uniformly-spaced knot subsequences and, according to [Dyn00], $C^k$ uniform interpolating schemes have to reproduce all polynomials of degree $k$. Consequently we used interpolants of degree at least $k$ for our $C^k$ constructions.

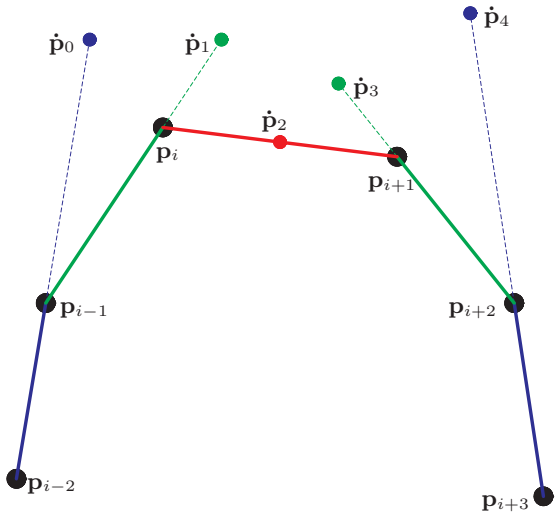


**Fig. 12.** Local linear interpolation yielding the auxiliary points for the 6-point scheme.

A more pedantic but precise naming is *constructive* interpolants of minimal degree since, somewhat surprisingly, the interpolating schemes of high continuity can be obtained using only linear interpolants! Specifically we can build from linear interpolants Warren's $C^2$ 6-point scheme (HERE originally local interpolating degree 5), our new $C^3$ 6-point scheme (degree 3) and the almost $C^4$ 8-point (degree 4). We conjecture that such formulas can also be found for the new 10-point scheme etc. But we rush to point out that, to find such linear-interpolation-based formulas, we first constructed a good scheme. To find good schemes from linear interpolants does not seem promising.

Formulas for symmetric $2n$-point schemes for linear interpolants (hence only half the formulas are needed) have the following construction (cf. Fig. 12). For a fixed $i$, we set

$$\dot{\mathbf{p}}_s := \mathbf{f}^1_{i-n+1+s}(\frac{1}{2}(t_i + t_{i+1})), \quad s = 0, \ldots, 2n-2 \tag{9}$$

and denote $\dot{\beta}_s := \beta_{i-n+1+s}$, $s = 1, \ldots, 2n-2$. Then the new point $\tilde{\mathbf{p}}_{2i+1}$ can be expressed via the following points $\dot{\mathbf{p}}_s$

$$\tilde{\mathbf{p}}_{2i+1} := \sum_{s=0}^{2n-2} \alpha_s \dot{\mathbf{p}}_s \text{with symmetry } \dot{\beta}_s \to (\dot{\beta}_{2n-1-s})^{-1} \Rightarrow \alpha_r \to \alpha_{2n-2-r}. \tag{10}$$

where for the uniform
4-point * $\alpha_0 := 2w$.
6-point $\alpha_0 := -\frac{2}{3}w$, $\alpha_1 := \frac{8}{3}w + \frac{1}{8}$.
8-point $\alpha_0 := \frac{2}{5}w$, $\alpha_1 := -\frac{12}{5}w - \frac{1}{128}$, $\alpha_2 := 6w + \frac{5}{32}$.
10-point $\alpha_0 := -\frac{2}{7}w$, $\alpha_1 := \frac{16}{7}w + \frac{1}{1024}$, $\alpha_2 := -8w - \frac{7}{512}$, $\alpha_3 := 16w + \frac{175}{1024}$.
(*linear interpolating functions are consistent with $C^1$).
As an example of a non-uniform scheme, for $\mathrm{CR}^2_{\mathrm{w}}$, the formulas are

$$\alpha_4 := -\frac{8w}{(1+\dot\beta_3)(1+\dot\beta_4)(1+2\dot\beta_3)},$$
$$\alpha_3 := \frac{(1+\dot\beta_2)(1+2\dot\beta_3)(1+\dot\beta_4)+32w(2+\dot\beta_2+2\dot\beta_3+\dot\beta_4+2\dot\beta_3\dot\beta_4}{4(1+\dot\beta_2)(1+\dot\beta_3)(1+\dot\beta_4)(1+2\dot\beta_3)}.$$

## 6 Conclusions

While uniform schemes can be constructed algebraically and analyzed with z-transforms (see for example [KLY07]), it is difficult to see a similar calculus for non-uniform schemes. And with a rigorous prediction of shape and curvature not even available for linear subdivision, it is not surprising that the more complicated non-linear setting does not provide proofs. Hence we shared observations and corresponding recipes.

Starting from $C^3$, interpolatory non-uniform subdivision rules are not only quite complex, but the shape is unsatisfactory both for highly non-uniform samples and, as for all curve constructions, for strong change in discrete curvature. While careful minimal interpolant-based constructions yield some progress they are still not satisfactory. An initial step of the simple 6-point scheme $\mathrm{CR}^2_{3/256}$, based on degree 2 interpolants, addresses non-uniform samples well. And strong change in discrete curvature can be handled by relaxing interpolatory requirements and possibly adding curvature-sensitive averaging.

**Acknowledgments.** The work was supported in part by NSF Grant CCF-1117695. We thank the referees. One referee pointed out an alternative construction for interpolants [BCR13] that appeared after our submission.

## References

[ADS10] Ursula H. Augsdörfer, Neil A. Dodgson, and Malcolm A. Sabin. Variations on the four-point subdivision scheme. *Computer Aided Geometric Design*, 27(1):78–95, 2010.

[BCR11a] Carolina Beccari, Giulio Casciola, and Lucia Romani. Polynomial-based non-uniform interpolatory subdivision with features control. *Journal of Computational and Applied Mathematics*, 16(235):47544769, 2011.

[BCR11b] Carolina Vittoria Beccari, Giulio Casciola, and Lucia Romani. Non-uniform interpolatory curve subdivision with edge parameters built upon compactly supported fundamental splines. *BIT Numerical Mathematics*, 51(4):781–808, 2011.

[BCR13] Carolina Vittoria Beccari, Giulio Casciola, and Lucia Romani. Construction and characterization of non-uniform local interpolating polynomial splines. *J. Computational Applied Mathematics*, 240, 2013.

[DFH04] Nira Dyn, Michael S. Floater, and Kai Hormann. A $C^2$ four-point subdivision scheme with fourth order accuracy and its extensions. In M. Daehlen, K. Morken, and L.L. Schumaker, editors, *Mathematical Methods for Curves and Surfaces, Tromsoe*, pages 145–156, 2004.

[DGS99] Ingrid Daubechies, Igor Guskov, and W. Sweldens. Regularity of irregular subdivision. *Constr. Approx.*, 15(3):381–426, 1999.

[DH12] Nira Dyn and Kai Hormann. Geometric conditions for tangent continuity of interpolatory planar subdivision curves. *Computer Aided Geometric Design*, 29(6):332–347, 2012.

[DL02] Nira Dyn and David Levin. Subdivision schemes in geometric modelling. *Acta Numerica*, 11:73–144, 2002.

[DLG88] N. Dyn, D. Levin, and J. Gregory. A 4-point interpolatory subdivision scheme for curve design. *Computer Aided Geometric Design*, 4(4):257–268, 1988.

[Dyn92] Nira Dyn. Subdivision schemes in computer-aided geometric design. In W Light, editor, *Advances in numerical analysis II*, pages 36–104. Oxford University Press, 1992.

[Dyn00] Nira Dyn. Interpolatory subdivision schemes. In A. Iske, E. Quak, and M.S. Floater, editors, *Tutorials on Multiresolurion in Geometric Modelling*, pages 25–50. Springer Verlag, Heidelberg, 2000.

[FBCR1x] M. Floater, Carolina Vittoria Beccari, T. Cashman, and Lucia Romani. A smoothness criterion for monotonicity-preserving subdivision. *Advances in Computational Mathematics*, 240, 201x.

[Hor12] Kai Hormann. private communication, October 2012.

[KLY07] Kwan Pyo Ko, Byung-Gook Lee, and Gang Joon Yoon. A study on the mask of interpolatory symmetric subdivision schemes. *Applied Mathematics and Computation*, 187(2):609–621, April 2007.

[KP12] K. Karčiauskas and J. Peters. Curvature-sensitive splines, 2012. presentation at: 8th Itl. conference on Mathematical Methods for Curves and Surfaces, Oslo, Norway.

[KP13a] K. Karčiauskas and J. Peters. Curvature-sensitive splines and design with basic curves. *Computer-Aided Design*, (45):415–423, 2013.

[KP13b] K. Karčiauskas and J. Peters. Non-uniform interpolatory subdivision via splines. *Journal of Computational and Applied Mathematics, MATA 2012 issue*, 240:31–41, 2013.

[Lan85] Serge Lang. *Complex Analysis*. Springer, New York, 2 edition, 1985.

[Lee89] E. Lee. Choosing nodes in parametric curve interpolation. *Computer Aided Design*, 21(6), 1989. Presented at the SIAM Applied Geometry meeting, Albany, N.Y., 1987.

[Sab10] M. Sabin. *Analysis and Design of Univariate Subdivision Schemes*, volume 6 of *Geometry and Computing*. Springer-Verlag, New York, 2010.

[SD05] Malcolm A. Sabin and Neil A. Dodgson. A circle-preserving variant of the four-point subdivision scheme. In *Mathematical Methods for Curves and Surfaces: Tromsø 2004, Modern Methods in Mathematics*, 2005.

[War95] J. Warren. Binary subdivision schemes for functions over irregular knot sequences. In Morten Dæhlen, Tom Lyche, and Larry L. Schumaker, editors, *Proceedings of the first Conference on Mathematical Methods for Curves and Surfaces (MMCS-94)*, pages 543–562, Nashville, USA, June 16–21 1995. Vanderbilt University Press.

[Wei90] A. Weissman. *A 6-point interpolatory subdivision scheme for curve design*. PhD thesis, Tel Aviv University, 1990.

# Appendix

## 6.1 Interlaced spline smoothing

Since formulas for $C^1$, $C^2$ and $C^3$ constructions appeared in [KP13b, Section 2], we list here only formulas for smoothness higher than $C^3$. Denote the Bézier control points of two consecutive curve segments of degree $m$, connected with geometric continuity parameter $\beta$, by $\tilde{\mathbf{b}}_0, \ldots, \tilde{\mathbf{b}}_m$, respectively $\mathbf{b}_0, \ldots, \mathbf{b}_m$, $\tilde{\mathbf{b}}_m = \mathbf{b}_0$. Each step modifies the $C^{k-1}$ constraint and enforces a new $C^k$ constraint.

*Smoothing $C^2 \to C^4$* The curves are assumed $C^2$ connected. We set (redefine)

$$\begin{aligned}
\mathbf{b}_3 :=& a_0\tilde{\mathbf{b}}_{m-4} + a_1\tilde{\mathbf{b}}_{m-2} + a_2\mathbf{b}_0 + a_3\mathbf{b}_2 + a_4\mathbf{b}_4 \ , \\
\mathbf{b}_{m-3} :=& \tilde{a}_0\tilde{\mathbf{b}}_{m-4} + \tilde{a}_1\tilde{\mathbf{b}}_{m-2} + \tilde{a}_2\mathbf{b}_0 + \tilde{a}_3\mathbf{b}_2 + \tilde{a}_4\mathbf{b}_4 \ , \\
a_0 :=& -\frac{\beta^4}{4(1+\beta)} \ , \ a_1 := \frac{1}{2}\beta^2(1+\beta) \ , \ a_2 := -\frac{1}{4}(1+\beta)^3 \ , \\
a_3 :=& 1+\beta \ , \ a_4 := \frac{1}{4(1+\beta)} \ ;
\end{aligned} \tag{11}$$

and $\tilde{a}_k(\beta) := a_{4-k}(\frac{1}{\beta})$, $k = 0, \ldots, 4$.

*Smoothing $C^3 \to C^5$* The curves are assumed $C^3$ connected. We set (redefine)

$$\begin{aligned}
\mathbf{b}_4 :=& a_0\tilde{\mathbf{b}}_{m-5} + a_1\tilde{\mathbf{b}}_{m-3} + a_2\tilde{\mathbf{b}}_{m-2} + a_3\mathbf{b}_2 + a_4\mathbf{b}_3 + a_5\mathbf{b}_5 \ , \\
\tilde{\mathbf{b}}_{m-4} :=& \tilde{a}_0\tilde{\mathbf{b}}_{m-5} + \tilde{a}_1\tilde{\mathbf{b}}_{m-3} + \tilde{a}_2\tilde{\mathbf{b}}_{m-2} + \tilde{a}_3\mathbf{b}_2 + \tilde{a}_4\mathbf{b}_3 + \tilde{a}_5\mathbf{b}_5 \ , \\
a_0 :=& \frac{\beta^5}{5(1+\beta)} \ , \ a_1 := -\frac{3}{5}\beta^3(1+\beta) \ , \ a_2 := \frac{2}{5}\beta^2(1+\beta)^2 \ , \\
a_3 :=& -\frac{3}{5}(1+\beta)^2 \ , \ a_4 := \frac{7}{5}(1+\beta) \ , \ a_5 := \frac{1}{5(1+\beta)};
\end{aligned} \tag{12}$$

and $\tilde{a}_k(\beta) := a_{5-k}(\frac{1}{\beta})$, $k = 0, \ldots, 5$.

## 6.2 Interpolatory subdivision replicating an underlying spline

Let $\mathbf{f}_i$ be pieces of the spline, of any continuity $\geq 0$, in Bézier form of degree $m$, defined over $[0\,..\,1]$.

- The spline is sampled at the points $\mathbf{f}_r(\frac{j}{m})$, $j = 0, \ldots, m$, $j = 0, \ldots, m-1$, ($\mathbf{f}_{r-1}(\frac{m}{m})$= $\mathbf{f}_r(\frac{0}{m})$). To the segment $\mathbf{f}_r(\frac{j}{m}), \mathbf{f}_r(\frac{j+1}{m})$ the label $j$ is assigned. Sampled points are denoted by $\mathbf{p}_i$ and the knot spacing $t_i$ is uniform.
- The new point with label $s$, corresponding to the segment $(\mathbf{p}_i, \mathbf{p}_{i+1})$, is the value at $\frac{t_i+t_{i+1}}{2}$ of the polynomial interpolant of degree $m$ to the points $\mathbf{p}_{i-s+j}$, $j = 0, \ldots, m$. The interpolant coincides with the initial $\mathbf{f}_r$ of this segment defined over interval $[t_{i-s}\,..\,t_{i-s+m}]$. Hence insertion rules indeed depend only on label $s$ and are easily pre-calculated.
- New subsegments are labeled $s$.

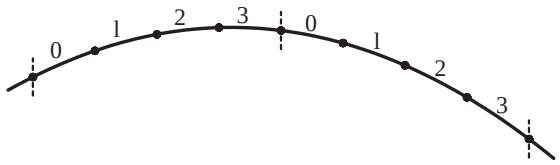


**Fig. 13.** Labelling the upsampled spline (case $m = 4$).

*Pre-calculation of insertion rules* We take Lagrange polynomial of degree $m$ interpolating at $i$ the points $\mathbf{p}_i$, $i = 0, \ldots, m$, and evaluate it at $s + \frac{1}{2}$. The coefficients for $\mathbf{p}_i$ form a mask of a new point corresponding to label $s$. Due to symmetry, only half the entries, $s = 0, \ldots, \frac{m}{2} - 1$, are displayed and the entries must be divided by $2^D$

$$
\begin{aligned}
m :=& 4: \qquad D = 7 \\
s :=& 0 \quad (35, 140, -70, 28, -5); \\
s :=& 1 \quad (-5, 60, 90, -20, 3). \\
m :=& 6: \qquad D = 10 \\
s :=& 0 \quad (231, 1386, -1155, -924, -495, 154, -21); \\
s :=& 1 \quad (-21, 378, 945, -420, 189, -54, 7); \\
s :=& 2 \quad (7, -70, 525, 700, -175, 42, -5)\ . \\
m :=& 8: \qquad D = 15 \\
s :=& 0 \quad (6435, 51480, -60060, 72072, -64350, 40040, -16380, 3960, -429); \\
s :=& 1 \quad (-429, 10296, 36036, -24024, 18018, -10296, 4004, -936, 99); \\
s :=& 2 \quad (99, -1320, 13860, 27720, -11550, 5544, -1980, 440, -45); \\
s :=& 3 \quad (-45, 504, -2940, 17640, 22050, -5880, 1764, -360, 35)\ .
\end{aligned}
$$